
Mixotrophic lifestyle of the ichthyotoxic haptophyte, *Prymnesium parvum*, offered different sources of phosphorus

Boucher Clémence ^{1,*}, Lacour Thomas ¹, André Julie ¹, Réveillon Damien ¹, Hansen Per Juel ², Mairé Francis ¹

¹ Ifremer, PHYTOX, Rue de l'Île d'Yeu, 44311 Nantes Cedex 03, France

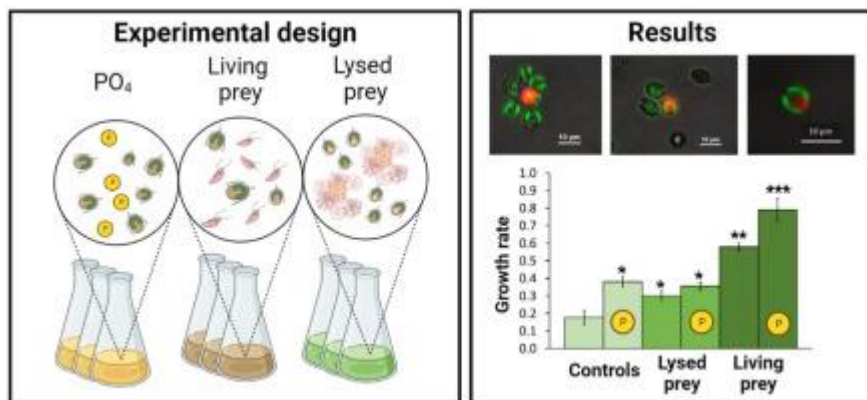
² University of Copenhagen, Department of Biology, Marine Biological Section, Strandpromenaden 5, 3000 Helsingør, Denmark

* Corresponding author : Clémence Lacour, email address : clemence.boucher@ifremer.fr

Abstract :

Many harmful algae are mixoplanktonic, i.e. they combine phototrophy and phagotrophy, and this ability may explain their ecological success, especially when environmental conditions are not optimal for autotrophic growth. In this study, laboratory experiments were conducted with the mixotrophic and ichthyotoxic haptophyte *Prymnesium parvum* (strain CCAP 946/6) to test the effects of phosphorus (P) sufficiency and deficiency on its growth rate, phagotrophic and lytic activities. P-deficient *P. parvum* cultures were grown without or with addition of P in the form of inorganic phosphorus (nutrients) and/or living algal prey (i.e. the cryptophyte *Teleaulax amphioxeia*). The ingestion rate of *P. parvum* and prey mortality rate were calculated using flow cytometry measurements based on pigment-derived fluorescence to distinguish between prey, predators and digesting predators. The first aim of the study was to develop a method taking into account the rate of digestion, allowing the calculation of ingestion rates over a two-week period. Growth rates of *P. parvum* were higher in the treatments with live prey, irrespective of the concentration of inorganic P, and maximum growth rates were found when both inorganic and organic P in form of prey were added (0.79 ± 0.07 d⁻¹). In addition, the mortality rate of *T. amphioxeia* induced by lytic compounds was 0.2 ± 0.02 d⁻¹ in the P-deficient treatment, while no mortality was observed under P-sufficiency in the present experiments. This study also revealed the mortality due to cell lysis exceeded that of prey ingestion. Therefore, additional experiments were conducted with lysed prey cells. When grown with debris from prey cells, the mean growth rate of *P. parvum* was similar to monocultures without additions of prey debris (0.30 ± 0.1 vs. 0.38 ± 0.03 d⁻¹), suggesting that *P. parvum* is able to grow on prey debris, but not as fast as with live prey. These results provide the first quantitative evidence over two weeks of experiment that ingestion of organic P in the form of living prey and/or debris of prey plays an important role in *P. parvum* growth and may explain its ecological success in a nutrient-limited environments.

Graphical abstract



Highlights

► Use of flow cytometry to quantify ingestion rate of the toxic mixoplankton *Prymnesium parvum*. ► Addition of algal prey significantly increased the growth rate of *P. parvum* both in inorganic [phosphorus deficiency](#) and sufficiency cultures. ► Rates of ingestion and the lytic effects were stimulated by inorganic phosphorus deficiency in *P. parvum*. ► *P. parvum* is able to use prey and/or debris derived from algae as phosphorus sources.

Keywords : *Prymnesium parvum*, Mixotrophy, Phagotrophy, Ingestion rate, Flow cytometry, Allelopathy

1. Introduction

The haptophyte *Prymnesium parvum* (N. Carter, 1937) is widely distributed and capable of forming blooms in both coastal and brackish inland water bodies (Baker et al., 2007; Roelke et al., 2016). This unicellular microalgae can produce toxins, called prymnesins, and other secondary metabolites to kill or inhibit the growth of other organisms, a process called allelopathy (Granéli & Salomon, 2010). This leads to Harmful Algal Blooms (HABs), which result in severe ecological and economic impacts in many areas around the world (Edvardsen & Paasche, 1998; Henrikson et al., 2010; Johnsen et al., 2010; Roelke et al., 2011, 2016). The most recent example is from the Oder River in Poland, in 2022, where a bloom of *P. parvum* caused the death of ~250 tons of fish (Marchowski & Ławicki, 2023). In this context, it is crucial to deepen our knowledge regarding the underlying factors that lead to the formation of these HABs.

P. parvum is a mixotrophic microalga, i.e. it is able to combine phototrophy and heterotrophy (phago and/or osmotrophy) to acquire energy and nutrients for its growth (Matantseva & Skarlato, 2013; Flynn et al., 2018). This nutrient strategy found in many toxic microalgae, allows them to grow under adverse conditions, which could explain their ecological success (Flynn et al., 2013; Mitra et al., 2014; Stoecker et al., 2017; Mitra et al., 2023). Phagotrophy among planktonic microalgae has long been considered an important adaptation to life in oligotrophic aquatic habitats (Hartmann et al., 2012; Nygaard & Tobiesen, 1993; Unrein et al., 2014). More recently, it has been recognised that mixotrophy is also important in eutrophic estuaries and coastal marine bays, especially among harmful bloom-forming microalgae (Adolf et al., 2008; Burkholder et al., 2008; Li et al., 2022). In these water bodies, mixotrophic microalgae feed directly on nutrient inputs and indirectly on algal prey.

Previous studies have shown that *P. parvum* feeds on other microalgae (e.g. *Dunaliella* sp., *Gyrodinium* sp., *Heterocapsa rotundata*, *Oxyrrhis marina*, *Rhodomonas salina*, *R. baltica*, diatoms) under both nutrient limiting and replete conditions (Tillmann, 1998; Granéli & Johansson, 2003b; Martin-Cereceda et al., 2003; Skovgaard & Hansen, 2003; Carvalho & Granéli, 2010; Lundgren et al., 2016; Cagle et al., 2021; Anestis et al., 2022). In addition, allelopathic compounds (likely prymnesins and other compounds), can affect other organisms by killing and lysing competitors (Fistarol et al., 2003; Barreiro et al., 2005; Uronen et al., 2005, 2007) and grazers (Skovgaard & Hansen, 2003; Blossom, 2014; Blossom et al., 2014; Cagle et al., 2021; Driscoll et al., 2023). Moreover, it is believed that the dissolved organic matter resulting from lysis of target cells/organisms becomes available in the medium and might be used as a nutrient source (Uronen et al., 2007). Hitherto, little is known about how nutritive conditions affect quantitatively the ingestion rate in *Prymnesium parvum*. In this context, one question that arises is which nutritive conditions lead to an increased growth rate or a higher phagotrophic activity in this species?

The methods usually used to estimate phagotrophy in mixotrophs are based on epifluorescence microscopy techniques with tracers such as live fluorescently labelled algae (Ferreira et al., 2022), fluorescent microspheres (Smalley et al., 1999; Legrand, 2001), the combination of microscopy and flow cytometry, using digestive vacuole markers such as LysoSensor, and/or the relative autofluorescence of the phycoerythrine (PE, found in cryptophytes) based on the disappearance of prey (Bowers et al., 2010; Carvalho & Granéli, 2010; Lundgren et al., 2016; Almada et al., 2017). Techniques using markers have an advantage over the addition of cryptophytes (using PE as a marker) in that a variety of prey can be used. However, the main limitation of these methods is that they may only be used over a very short time of experiment (when digestion can be neglected) or from long term responses, typically

ignoring the digestion of prey cells or the lysis of prey cells due to allelopathy, which then leads to overestimation of ingestion rates.

Thus, the first aim of this study was to develop a method to quantify the ingestion rates of *P. parvum* (CCAP 946/6 strain) taking into account the digestion rate, using a combination of flow cytometer and microscopic observations. In a second part of this study, we investigated the effects of phosphorus sufficiency and deficiency on its growth rate, abundance, lytic and phagotrophic activities. Thus, we tested the hypotheses that (1) the addition of algal prey (i.e. the cryptophyte *Teleaulax amphioxeia*) will allow *P. parvum* to grow under phosphorus deficiency with the same rate as with the presence of inorganic phosphorus (IP); (2) The addition of both, living prey and IP, in the medium will allow *P. parvum* to achieve the same growth rate as under conditions with only prey or IP, and (3) *P. parvum* may produce allelopathic compounds that kill its prey especially in P-deficient conditions. Finally, we hypothesized that (4) *P. parvum* may exploit debris, derived from freshly killed prey, to grow under IP deficiency conditions. In the present study, the ingestion of organic P in the form of live prey and/or prey debris was quantitatively assessed and highlighted the important role of phagotrophy in the growth rate of *P. parvum* that may explain its efficiency in forming blooms

2. Materials and methods

2.2. Algal cultures

Axenic culture of the haptophyte *Prymnesium parvum* (strain CCAP 946/6; Culture Collection of Algae and Protozoa; 8 to 14 μm long \times 5 to 10 μm wide) and non-axenic culture of the cryptophyte *Teleaulax amphioxeia* (strain AND-A0710; 7-10 μm long and 4-6 μm wide) were used as predator and prey, respectively. These two strains were routinely grown using batch cultures in L1 medium without silicate (Guillard and Hargraves, 1993), prepared with 0.2 μm -filtered seawater (salinity 35). Cultures were maintained at $17 \pm 1^\circ\text{C}$, at an irradiance of $45 \mu\text{mol photons m}^{-2} \text{s}^{-1}$ provided by cool-white and pink fluorescent tubes (12:12 h, light:dark cycle).

2.3. Experimental design

Experiments started when the stock cultures of both prey and predator reached stationary growth phase (i. e. highest cell density) and were deficient in phosphorus (i. e. no phosphorus was detected). Cultures of *P. parvum* were gradually deficient in inorganic phosphorus (IP) for 3 weeks before the experiment began and medium was freshly supplemented with L1 completely deficient in IP, one week beforehand, to ensure that other elements were not limiting. The *T. amphioxeia* culture was used after 7 days, when IP was limiting in the medium. We confirmed the absence of IP (see method below) in both *T. amphioxeia* and *P. parvum* inoculums. All experimental cultures were grown in triplicates at $17 \pm 1^\circ\text{C}$ and at an irradiance of $45 \mu\text{mol photons m}^{-2} \text{s}^{-1}$ for up to 16 days.

2.3.1. Experiment 1: Detection of phagotrophic activity of *P. parvum* using flow cytometry and microscopy

A method was developed to demonstrate the ability of *P. parvum* to ingest live *T. amphioxeia* cells using a combination of FACS and microscopic observations. Mixed cultures with *P. parvum* cells and living prey were analyzed and sorted after 72h of exposure, with a sorting flow cytometer. Cell sorting was carried out using a BD FACS ARIA III flow cytometer (Cytocell platform) equipped with a 488 nm argon ion laser (blue laser). Upon excitation by the laser, PE and Chl *a* autofluorescence were detected with 585/42 nm filter (FL2) and 695/40 nm filter (FL3), respectively. On cytograms, four populations appeared, which were sorted at high pressure using a 100- μ m nozzle, a drop drive frequency of 30 kHz and a flow rate of 300 cells s⁻¹. Each collected population was observed with a Nikon A1Rs confocal laser scanning microscope (MicroPicell Platform) for identification. Fluorescence emitted by pigment was investigated using an argon laser (488 nm) and a superposition of filters. Pictures and video (Suppl.) of cells were taken using NIS Elements Software.

2.3.2. Experiment 2: mixed culture with living prey

To investigate the ability of *P. parvum* to exploit different sources of phosphorus, we grew previously IP-starved cells in L1 medium (882 μ M NO₃⁻, trace minerals and vitamins) with or without addition of IP (36 μ M PO₄³⁻) “**Ctrl +IP**” and “**Ctrl -IP**”, respectively, and in combination with the presence or absence of algal prey (i.e. the cryptophyte *Teleaulax amphioxeia*), “**Prey +IP**” and “**Prey -IP**” (fig. 1). Each treatment consisted of an IP-starved *P. parvum* culture at an initial cell density of 10⁴ cells mL⁻¹. In mixed culture, the prey was added at a prey:predator ratio of 30:1 (i.e. initial prey cell density of 3 x 10⁵ cells mL⁻¹). IP-starved *T. amphioxeia* monocultures were also monitored throughout those experiments as controls, with or without addition of IP (36 μ M PO₄³⁻) “**Ctrl +IP**” and “**Ctrl -IP**”, respectively (fig. 1).

2.3.3. Experiment 3: monocultures with prey debris

This experiment was carried out to investigate if *P. parvum* cells were able to grow using debris derived from *T. amphioxeia*, in the presence or absence of inorganic phosphorus “**Debris +IP**” and “**Debris -IP**” (fig. 1). An IP-starved *T. amphioxeia* culture was centrifuged (20 min at 4°C and 4600g), resuspended in 10 mL of culture medium and sonicated using a VCX 500 sonicator with 3 mm diameter conical microprobes at very high intensity (amplitude 30%, 15', pulse mode 10 s ON, 5 s OFF). Microscopic observations confirmed the efficient cell lysis. In *P. parvum* culture exposed to debris, we added a *T. amphioxeia* lysate equivalent to a prey:predator ratio of 15:1.

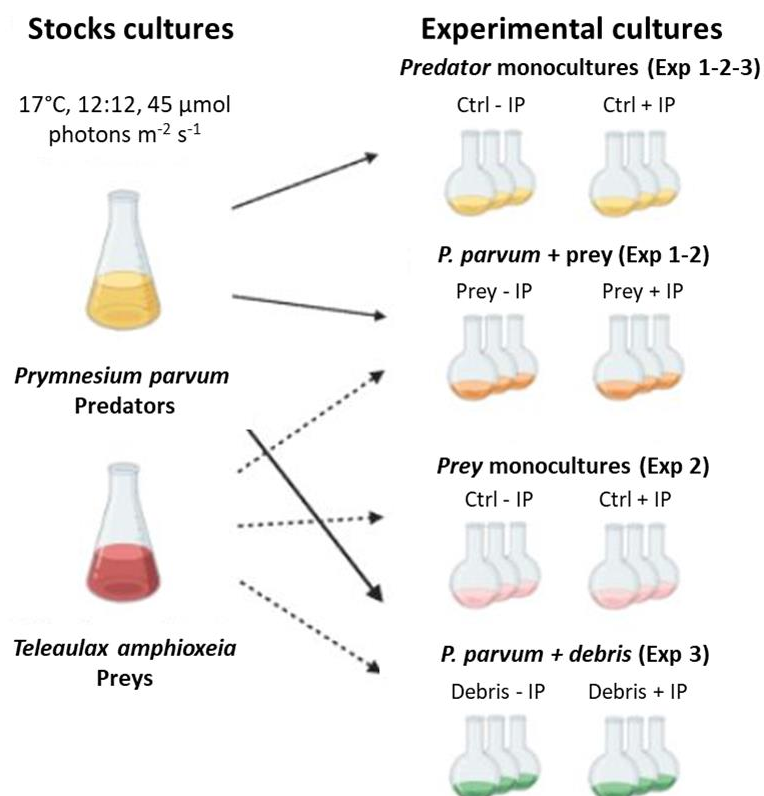


Fig 1. Schematic representation of the experiments (Exp 1-2-3). IP-starved stock cultures of *Prymnesium parvum* (predator) and *Teleaulax amphioxeia* (prey) were inoculated to achieve the following treatments: in absence or presence of inorganic

phosphorus (“-/+IP”) in presence or absence of algal prey (“Prey”) or debris of prey (“Debris”).

2.4. Analytical procedures

2.4.1. Flow cytometry measurements

All cells were enumerated using a MACSQUANT 10 cytometer (Miltenyi) with an excitation at 488 nm (blue laser). The cells were gated based on their size, shape and cell structural complexity (granularity) using forward scatter (FSC) and side scatter (SSC) light, respectively. In addition, two filters allowed to measure relative cell autofluorescence. The primary photosynthetic pigment, chlorophyll a (Chl a), found in both microalgae, emits light in the red-far red spectral range (>650 nm). Therefore, red fluorescence (B3H) was detected through a 655-730 nm filter. Whereas phycoerythrin (PE), found in *T. amphioxeia*, has a maximal fluorescence intensity at 575/25 nm. Hence, orange fluorescence (B2H) was collected through a 585/40 nm filter. *P. parvum* cells which had ingested *T. amphioxeia* cells gained an orange fluorescence signal (PE) which enabled to distinguish and count them separately. Subsamples were taken from each replicate at the beginning of experiments and then daily at a fixed time.

2.4.2. Cell counts and growth rate

Daily enumeration of *P. parvum* and *T. amphioxeia* was directly performed on fresh samples. Growth rates (d^{-1}) were calculated as follows:

$$\mu = \frac{\ln\left(\frac{D_{i+1}}{D_i}\right)}{t_{i+1} - t_i}$$

Where D_{i+1} and D_i are the cell density (cells mL⁻¹) of two consecutive measurements, at time t_{i+1} and t_i (day) respectively. Growth rates were averaged over 5 days (day 2 to 7, statistical data can be found in the Suppl. tab. 1).

2.4.3. Nutrient analyses, P content and uptake rate

Inorganic phosphorus (IP) as well as dissolved organic phosphorus (DOP) and particulate phosphorus (PP) were measured during the third experiment. For PP, cells from 10-20 mL of culture were collected on pre-combusted (450°C, 4h) Whatman GF/C filters into acid washed tubes. Filters and filtrates were stored at -80°C until oxidation. The oxidation and preparation of the oxidizing reagent were carried out according to the method of Pujo-Pay and Raimbault (1994). Phosphate concentrations were then determined with AXFLOW analysis. The intracellular phosphorus quotas per *P. parvum* cell were computed dividing PP concentration by *P. parvum* cell density. Rates of inorganic phosphorus (IP) uptake for the “Ctrl +IP” and “Debris +IP” treatments were calculated as follows:

$$Uptake\ rate = - \frac{d[IP]}{D_{Pp} dt}$$

where D_{Pp} is the cell density (cells L⁻¹) of *P. parvum* in the corresponding culture.

2.4.4. Feeding activity

A conceptual model was constructed to estimate the ingestion and digestion rates of *P. parvum* (called respectively ρ and λ , tab. 1). It was carried out to assess the contribution of phagotrophic activity on the growth rate of *P. parvum*. In this model, we assumed that a *P. parvum* cell can only ingest one prey at a time (in agreement with microscopic observations), and that the digestion rate is constant. Under these assumptions, the dynamic of the digesting cell concentration F is given by:

$$\frac{dF}{dt} = \rho D_{pp} - \lambda F.$$

Note that we also consider that if a digesting cell divides, the prey remains in one of the two daughter cells, so cell division does not affect the number of digesting cells.

In absence of prey, the ingestion rate is null so we get $F(t) = F_0 e^{-\lambda t}$. The digestion rate λ was thus estimated by fitting an exponential curve on the concentration of digesting cells (see section 2.3.1) over the period when the prey has disappeared (Suppl. fig. 2). Then, the ingestion rate was estimated over the whole experiments as follows:

$$\rho(t) = \frac{\frac{dF}{dt} + \lambda F}{D_{pp}},$$

using smoothing splines on F and D_{pp} (UnivariateSpline function in SciPy, Python 3) to reduce the noise and calculate the derivative.

2.4.5. Prey mortality

The mortality (M) of the prey *T. amphioxeia* was calculated as the percentage of intact cells exposed to *P. parvum* compared to the corresponding control (Ctrl +IP/-IP):

$$M = \frac{D_{ctrl} - D_{prey}}{D_{ctrl}} * 100$$

where “ D_{ctrl} ” is the cell density of *T. amphioxeia* in the corresponding control (Ctrl +IP/-IP) and “ D_{prey} ” the concentration of *T. amphioxeia* in the treatment (Prey +IP/-IP).

The mortality of *T. amphioxeia* may be due to ingestion by *P. parvum* or the effects of its toxins (or other compounds). To quantify the mortality rate (m) of each phenomenon, we consider, for both conditions (Prey +IP/-IP), the net specific growth

rate of *T. amphioxeia* (μ_{prey}) measured in the treatment is equal to the specific growth rate of the control (μ_{ctrl}) minus the mortality:

$$\mu_{prey} = \mu_{ctrl} - m_{ing} - m_{tox}$$

where m_{ing} and m_{tox} are the mortality rates due to ingestion and toxins, respectively.

The former can be computed from the ingestion rate (ρ), as follows:

$$m_{ing} = \frac{D_{Pp}}{D_{prey}} * \rho$$

After computing the growth rate of *T. amphioxeia* in the “Prey +IP/-IP” and the “Ctrl +IP/-IP”, we can finally estimate the toxin-induced mortality rate:

$$m_{tox} = \mu_{ctrl} - \mu_{prey} - m_{ing}$$

Table 1. Variable description used for the model and calculations.

Symbol	Description	Unit
D	Cell density of prey or <i>Pp</i>	cells mL ⁻¹
F	<i>P. parvum</i> cell with PE (Feeding cells)	cells mL ⁻¹
λ	Digestion rate	d ⁻¹
ρ	Ingestion rate	cell <i>prey</i> (cell <i>Pp</i> d) ⁻¹
μ	Specific growth rate	d ⁻¹
M	Mortality of <i>T. amphioxeia</i> (prey)	%
m	Mortality rate induced by toxins/ingestion	d ⁻¹

2.5. Statistical analyses

All statistical analyses were performed with R Studio 4.2.0. Normality and homoscedasticity of the residuals of the ANOVA (Analysis of Variance) were assessed with Shapiro-Wilk test and Bartlett test, respectively. One-way ANOVA was used to compare differences between treatments on growth rates of *P. parvum*. When significant, the ANOVA was followed by Tukey’s HSD post-hoc test. Differences were

considered significant when p -value < 0.05 . All values were reported as average of triplicates and expressed as mean \pm standard deviation (SD).

3. Results

3.1. Identification of phagotrophic activity in *Prymnesium parvum* using flow cytometry (Exp. 1)

The aim of this experiment was to demonstrate the ability of *P. parvum* to ingest live *T. amphioxeia* cells using a combination of FACS and microscopic observations. In the cytograms, *P. parvum* cells exhibited higher chlorophyll a (Chl a) relative fluorescence intensity than *T. amphioxeia*, and showed no phycoerythrin (PE) relative fluorescence (see section 1.3.1 and fig. 2A and B). This allowed for an easy separation of the two species. In mixed cultures, at $t=24$ h, a population appeared between the ones of *P. parvum* and of *T. amphioxeia* on the cytogram (fig. 2C). This group of cells had a Chl a fluorescence equal to the one of *P. parvum*, but with a higher PE fluorescence. Simultaneously, a high proportion of dead cells with lower PE and Chl a fluorescences was observed. These populations were sorted by FACS and imaged using confocal microscopy (fig 2, 1-3). The population between *P. parvum* and *T. amphioxeia* appeared to be *P. parvum* cells with a high PE fluorescence, (fig. 2, 3), providing evidence that this population of *P. parvum* had ingested *T. amphioxeia*. This process of ingestion was also captured by confocal microscopy (see Suppl. Movie).

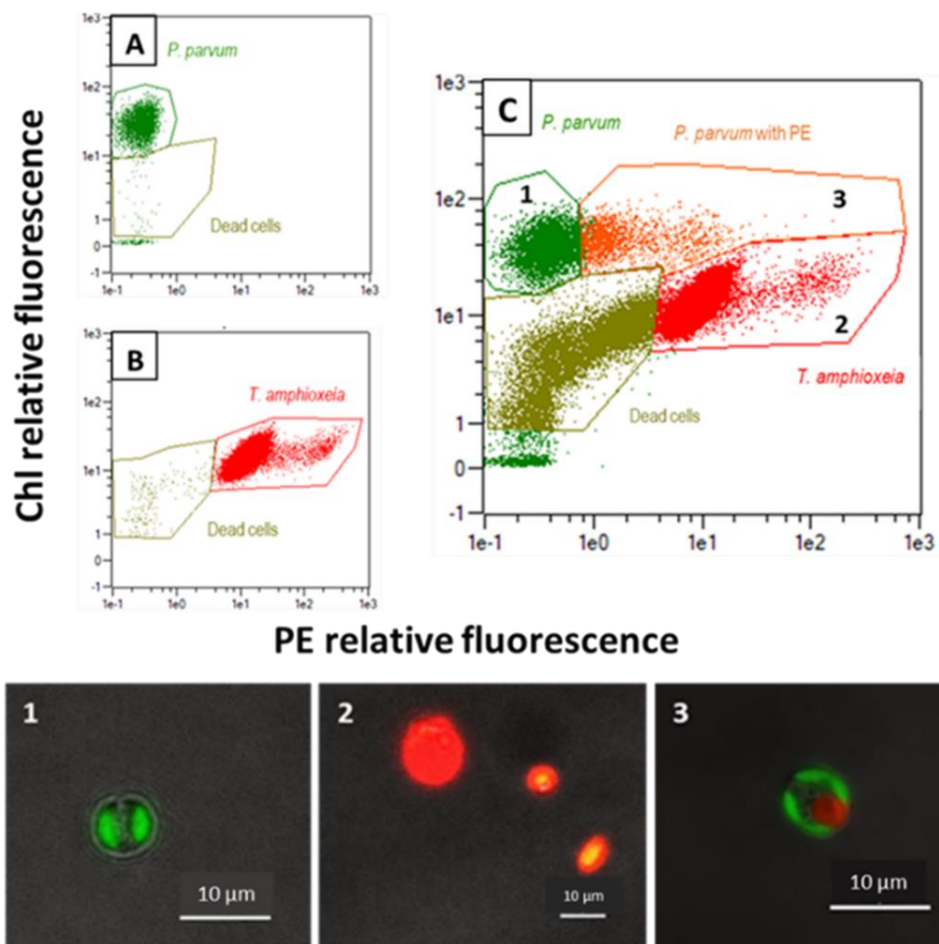


Fig. 2. Cytograms (upper-panel) and epifluorescence micrographs (lower panel) of monocultures of (A) *P. parvum* and (B) *T. amphioxeia* and (C) mixed culture of (1) *Prymnesium parvum* with (2) *Teleaulax amphioxeia* and in between (3) *P. parvum* containing one *T. amphioxeia* cell. Cells were observed under Nikon A1RS confocal microscope after cell sorting with a FACS ARIA III flow cytometer (see section 1.2.1).

3.2. Effect of phosphorus source on *Prymnesium parvum* growth, ingestion and prey mortality (Exp. 2)

The ability of *P. parvum*, which had depleted the inorganic phosphorous (IP) in the culture medium, to exploit different sources of phosphorus was tested in two treatments: 1) **Control** with and without inorganic phosphorus addition (Ctrl +IP and Ctrl –IP, respectively), 2) **Living prey** with and without addition of IP (Prey +IP and Prey –IP, respectively). The growth rates of *T. amphioxeia* were also monitored

throughout those experiments: 1) **Control** and 2) **Living prey**. Specific growth rates of *P. parvum* were always higher in the treatments with live prey compared to monocultures, irrespective of the presence or absence of inorganic phosphorous (fig. 3). In fact, the growth rate in the Prey -IP treatment was significantly higher than in the Ctrl -IP treatment (0.58 ± 0.02 vs. 0.21 ± 0.06 d⁻¹, p-value = 4×10^{-3}). The maximum growth rate was obtained in the Prey +IP treatment (0.79 ± 0.07 d⁻¹, p-value = 1×10^{-5}).

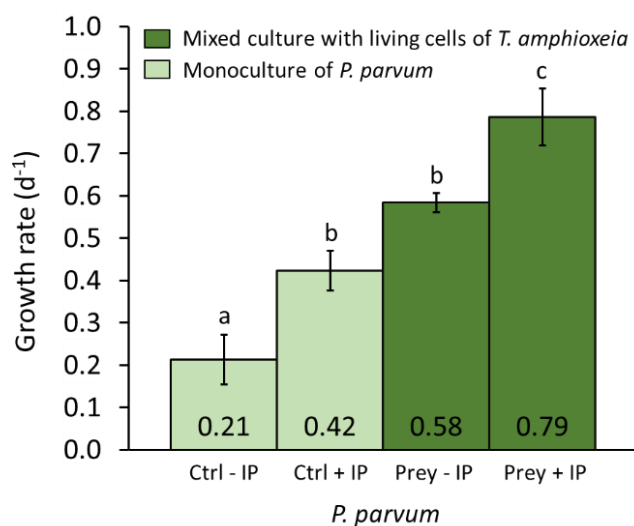


Fig. 3. Cell-specific growth rates (μ , d⁻¹) of *Prymnesium parvum* over 5 days (day 2 to 7) in monoculture with and without inorganic phosphorus (Ctrl +IP/-IP), and with living prey in presence or absence of inorganic phosphorus (Prey +IP/ -IP). Values are mean \pm SD, n = 3, letters represent a significant difference, p < 0.05.

The fraction of feeding *P. parvum* cells reached a maximum of 26 ± 1.2 % and 36 ± 1.4 % on day 2 in the Prey +IP and Prey -IP treatments, respectively (fig. 4A). A conceptual model was constructed to estimate the ingestion and digestion rates of *P. parvum* from the number of cells containing prey (see section 1.3.4). Focusing on the period when there is no more prey in the Prey -IP treatment, a digestion rate of 0.66 d⁻¹ was observed (see Suppl. fig 2). Assuming that this rate is constant, we obtained a higher initial prey ingestion rate in the Prey -IP treatment, compared to the Prey +IP

treatment. Maximum ingestion rate was obtained on the first day in the Prey – IP treatment (0.45 ± 0.04 prey $Pp^{-1} d^{-1}$; fig 4B). The observed declines in the ingestion rate after day 5 were related with the prey disappearance.

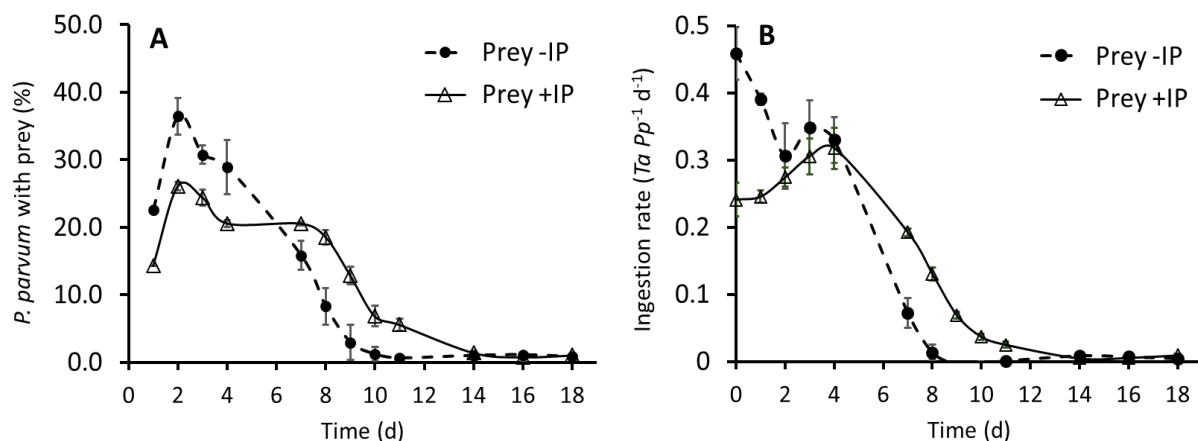


Fig 4. (A) Fraction of *Prymnesium parvum* cells containing prey (i.e. the cryptophyte *Teleaulax amphioxeia*) and (B) ingestion rate (prey $Pp^{-1} d^{-1}$) in the Prey –IP and Prey +IP treatments. Phagotrophy was detected based on the autofluorescence of phycoerythrin (PE) of the prey. Values are mean \pm SD, n = 3.

The dynamics of *T. amphioxeia* cell density results from its growth, its ingestion and from its mortality (i.e. lytic effects of *P. parvum*, see section 1.3.5). *T. amphioxeia* cell densities were monitored throughout experiment 2 (Suppl., fig. 1). The growth rate of *T. amphioxeia* in the mixed cultures with inorganic phosphorus (Prey +IP) was twice as low as control in the presence of IP (Ctrl +IP; 0.16 ± 0.02 and 0.32 ± 0.01 , p-value = $2 \cdot 10^{-3}$; fig. 5A). No growth was observed when exposed to IP-starved culture of *P. parvum* (Prey –IP, fig. 5A). Moreover, when grown in Prey -IP treatment, *T. amphioxeia* showed a total mortality of 91 ± 2.6 % at a *P. parvum* cell density of 3×10^5 cells mL^{-1} (day 7), while in Prey +IP treatment a similar mortality was not seen before the *P. parvum* culture had reached a cell density of $\sim 1.2 \times 10^6$ cells mL^{-1} after 2 weeks (fig. 5B, Suppl. fig 1). The mortality rates in presence of *P. parvum*, computed in

comparison with the control, were assumed to be due to ingestion and toxins (i.e. lytic effects). The main cause of mortality of *T. amphioxeia* was the lytic effect in both treatments (fig 5, C-D), which was markedly higher in the –IP treatment. In this treatment, lytic activity is present from day 0, whereas in the +IP treatment, no lytic activity is observed before day 2. However, the lower lytic activity of *P. parvum* in the +IP treatment despite higher *P. parvum* concentrations, is counterbalanced by the higher concentration of *T. amphioxeia* in the medium from day 2 (fig. 5; Suppl., fig. 1).

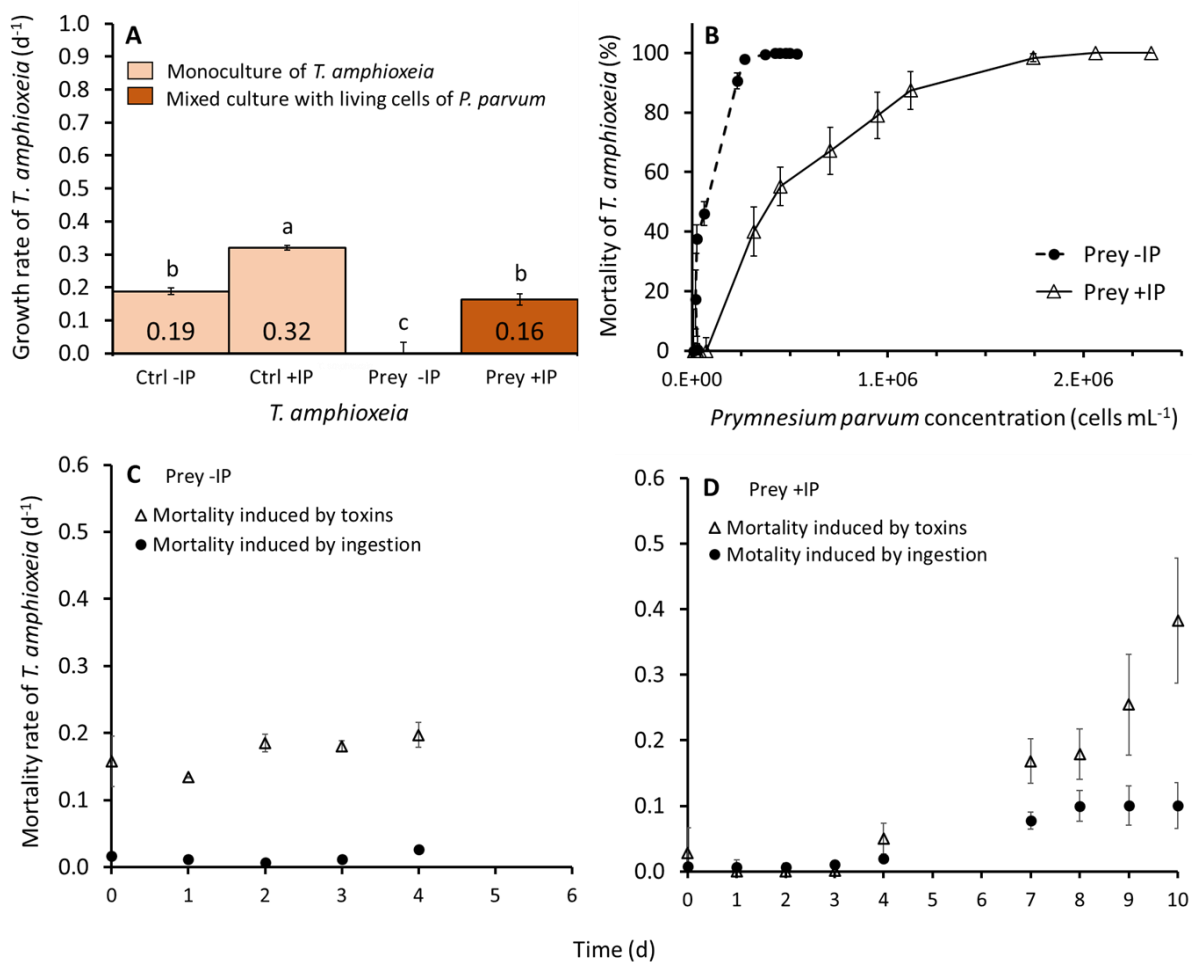


Fig. 5. *Teleaulax amphioxeia* (A) specific growth rate over 5 days (day 2 to 7) in monoculture with and without inorganic phosphorus (Ctrl +IP/–IP), and in mixed culture in presence or absence of IP (Prey +IP/–IP) and (B) percentage of mortality of the prey. Mortality rates induced by toxins (triangle) or ingestion (solid circle) in the (C)

“Prey –IP” treatment and (D) “Prey +IP” treatment, according to the time of experiment. Only dots where prey were high enough in the culture were plotted (for mortality rates calculations, see section 1.4.4). Values are mean \pm SD, n = 3; letters represent a significant difference, $p < 0.05$.

3.3. Ability of *Prymnesium parvum* to exploit debris for growth (Exp. 3)

The lysis of prey cells generated debris (fig. 2) that could have released organic and inorganic phosphorus and other nutrient/organic matter used by *P. parvum* to grow. Thus, another experiment was carried out to investigate if IP-starved *P. parvum* cells were able to grow from dead cells of *T. amphioxeia* based on two treatments: 1) **Control** with and without inorganic phosphorus addition (Ctrl +IP/–IP, respectively) and 2) **Prey debris** with and without IP addition (Debris +IP/–IP). Specific growth rate of *P. parvum* were similar when grown with prey debris (Debris -IP) as in the control with addition of inorganic phosphorus (Ctrl +IP) (0.30 ± 0.1 vs. 0.38 ± 0.04 d⁻¹, p-value = 0.67) (fig. 6). Thus, the addition of phosphorus in the form of prey debris is sufficient to support growth at the same level as in the form of inorganic nutrients. Finally, the “Debris –IP” and “Debris +IP” treatments were not significantly different (0.30 ± 0.04 vs. 0.36 ± 0.02 d⁻¹, p-value = 0.99) and cell densities were similar (Suppl., fig. 1). Hence, for *P. parvum* cultures in the presence of IP, the addition of debris does not increase growth compared to cultures with only IP or only debris. However, it is not possible to distinguish here whether the growth is related to debris or to IP.

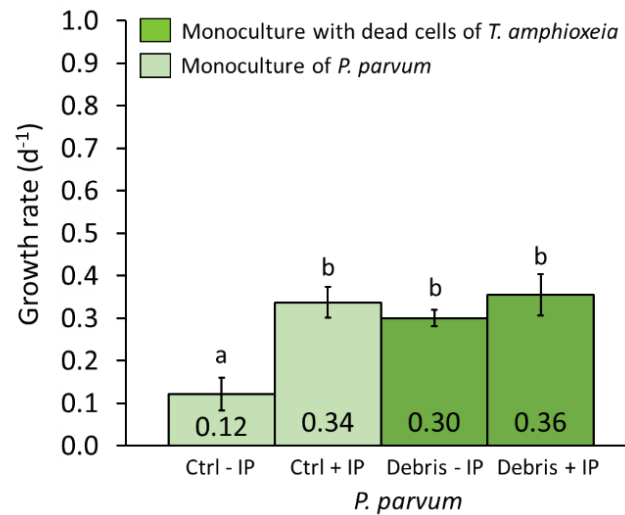


Fig. 6. Cell-specific growth rates (μ , d^{-1}) of *Prymnesium parvum* over 5 days (day 2 to 7) in monoculture with and without inorganic phosphorus (Ctrl +IP/-IP) and with debris of *Teleaulax amphioxeia* with or without inorganic phosphorus, (Debris +IP/-IP). Values are mean \pm SD, $n = 3$, letters represent a significant difference, $p < 0.05$.

To evaluate the physiological status of *P. parvum* when grown on debris, its intracellular phosphorus quota was monitored for each treatment (fig. 7A). Data prior to day 8 are not presented here, as at this time it was not possible to separate phosphorus from debris and phosphorus from intracellular *P. parvum*, as both were retained on the filters. From day 8 onwards, none of the debris remained in the medium as it was either consumed or degraded, hence only the *P. parvum* cells were on the filter. In the presence of inorganic phosphorus in the Ctrl and Debris treatments, from day 8, the quota of *P. parvum* was constant throughout the experiment (fig. 7A) and close to its maximum ($27.5 \text{ fmol cell}^{-1}$, measured in a preliminary experiment) without significant differences between treatments. In the Debris -IP treatment, the intracellular phosphorus quota of *P. parvum* was lower and decreased over time, getting closer to its minimum quota ($3.70 \text{ fmol cell}^{-1}$, also measured in a preliminary experiment) (fig. 7A). These results show that, from day 8, phosphorus was limiting

growth only in the Debris -IP treatment. In this condition, the debris correspond to a phosphorus input of $\sim 4 \mu\text{M}$. Given that $1.20 \times 10^9 \text{ cells mL}^{-1}$ have been produced and assuming conservatively that they reach the minimum quota, at least $4 \mu\text{M}$ have been used, showing that all the phosphorus from the debris have been exploited.

In order to find out whether P was consumed in the form of debris or phosphate in the Debris +IP treatment, the uptake rate of inorganic P was plotted (fig. 7B). The results show that in the treatment with Debris, uptake of IP is lower than in the Ctrl condition while growth rates and P quotas were roughly similar. These results suggest that *P. parvum* consumes both sources of P for growth when present in the medium.

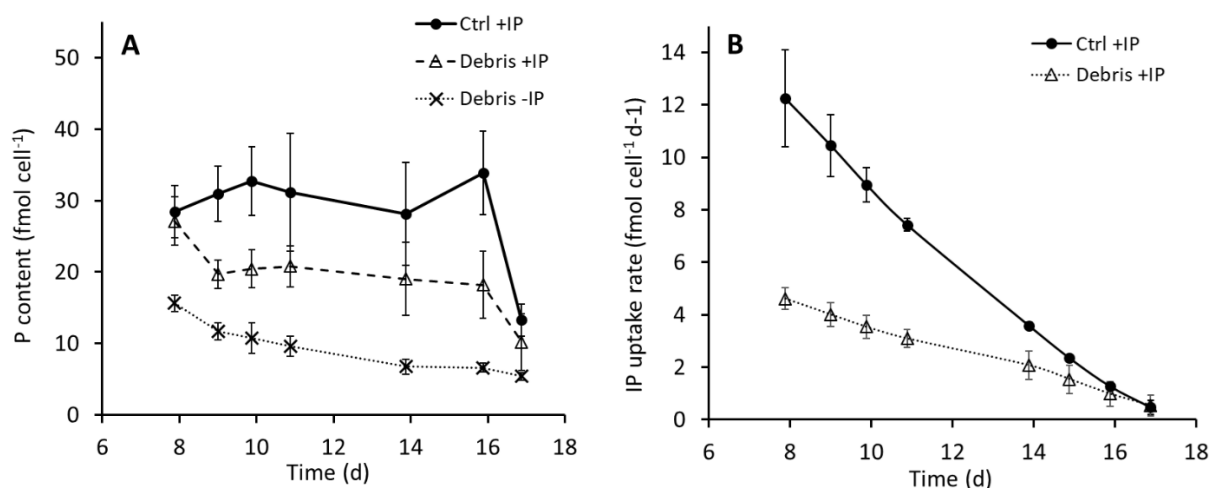


Fig 7. *Prymnesium parvum* (A) intracellular phosphorus quota (fmol cell⁻¹) in a monoculture of *Prymnesium parvum* with the addition of inorganic phosphorus (Ctrl +IP), and with debris of *Teleaulax amphioxeia* with or without IP (Debris +IP, Debris – IP) and (B) uptake rate of IP in “Ctrl +IP” and “Debris +IP” treatments. Values are mean \pm SD, n = 3 (for calculations of *P. parvum* quota and uptake rate, see section 1.4.2).

4. Discussion

How to quantify prey ingestion by *P. parvum*?

Published ingestion rates by *P. parvum* using a range of prey items and a variety of methods vary considerably (see table 2). Some of these differences may be due to intra-specific variability (since the strains are different) or related to a prey specificity or preference. However, the majority of the variability is most likely due to the method used to measure and calculate the ingestion rates.

Prey ingestion in phagotrophic protists can be measured using the reduction in prey cell density in mixed cultures of a prey and a predator as compared to control cultures of the prey (see table 2). This is very difficult in the case of *P. parvum*, since it releases lytic compounds, which lyse the prey cells above a certain threshold concentration of *P. parvum* (Skovgaard & Hansen, 2003; Medić et al., 2022; Anestis et al., 2022). To overcome this problem, killed prey particles have been used. However, these may not be taken up at the same rate as live prey (Beisner et al., 2019). Other studies have applied different techniques that score the increase in prey particles inside food vacuoles as a function of incubation time to estimate ingestion rates. The drawbacks of most previous attempts to measure rates of phagotrophy in *P. parvum* is that they rely on short term experiments using the addition of prey that can be tracked inside the *P. parvum* cells using fluorescence microscopy and/or flow cytometry (see table 2). Often *P. parvum* has not been acclimated to the prey added, and thus the experiments only last a few hours. This has led to dramatically different ingestion rates depending on the method and assumptions for calculations used (see table 2).

Our data indicated ingestion rates of *P. parvum* of roughly 0.3 prey $Pp^{-1} d^{-1}$ using the cryptophyte *Teleaulax amphioxeia* as a prey. This ingestion rate is far lower than

ingestion rates of *P. parvum* reported in several previous studies using cryptophyte prey (see Table 2). For instance, Carvalho & Granéli (2010) computed an ingestion rate of 9.6 prey $Pp^{-1} d^{-1}$ with a feeding frequency of *P. parvum* of 20 %. Following these data, the concentration of prey cells during the first 12 hours should have decreased substantially, whereas it remains constant during this period and similar to the control. This gap between values suggests that ingestion rates may be often overestimated due to methodological biases in the way rates were calculated. Actually, the ingestion rates expressed as biovolume ($> 10 \mu\text{m}^3 \cdot \mu\text{m}^{-3} \cdot \text{d}^{-1}$) are often much higher than the specific growth rate ($< 1 d^{-1}$), indicating an unlikely excessive consumption or reflecting a transient response. In Lundgren et al. (2016), ingestion rates were not calculated directly, as it was not possible to distinguish between mortality induced by cell lysis and by ingestion. Thus, the results here are given in terms of mortality rates incorporating both factors, which does not provide a good approximation of phagotrophic activity.

In the present study, *T. amphioxeia* was used as a prey because of its pigment composition (see method section 2.4.1) and because this cryptophyte is widely distributed from coastal to oceanic waters (Yoo et al., 2017). In fact, the concentration of *P. parvum* feeding cells was estimated thanks to the PE fluorescence signal of the prey found in *P. parvum* cells. The ingestion and digestion rates were then estimated from the dynamics of the feeding cell concentration, assuming a constant digestion rate. This assumption needs to be confirmed with more detailed experimental data, particularly as the digestion rate was calculated from a specific nutrient condition (phosphorus deficiency). Nevertheless, given that our method takes digestion into account, it is possible to measure ingestion over a two-week period, when the mixotrophic alga is used to the presence of prey. Moreover, the addition of prey that

possesses PE does not require manipulation prior to use, preys are alive and the fluorescence is stable over time compared to tracers that are photosensitive and for which the fluorescence disappears after a few hours. Finally, it was possible to make the distinction between prey mortality induced by lytic compounds and that due to *P. parvum* ingestion. Our method can thus be applied to other mixotrophic algae, as long as it is possible to distinguish them in flow cytometry by pigment composition (i.e. fluorescence). Moreover, the calculated ingestion rates can be used to estimate the phagotrophy-related traits of the species (e.g. the maximal ingestion rate and the half saturation constant) and finally to provide input for the existing models used to predict blooms (Edwards, 2019; Litchman, 2023; Mitra et al., 2023).

Table 2. Exhaustive table of studies on the phagotrophic activity of *P. parvum* in which ingestion rates have been estimated (reporting the highest values; biovolume of *P. parvum* is 180 μm^3).

<i>P. parvum</i> strain	Method	Prey	Biovolume of the prey (μm^3)	Nutritive condition	IR (prey. <i>Pp</i> ¹ . h ⁻¹)	IR ($\mu\text{m}^3.\mu\text{m}^{-3}.\text{d}^{-1}$)	Time of experiment (h)	Reference		
CCAP 946/6	FC ⁶ using PE ²	<i>Teleaulax amphioxeia</i>	113	P deficient P sufficient	0.02 0.01	0.30 0.20	288	This study		
KAC 39	FC ⁶ using PE ² and markers	<i>Rhodomonas salina</i>	268	Low NP Low N Low P	0.4* 0.4* 0.3*	14.0 14.0 10.5	4	Lundgren et al., (2016)		
KAC 39	FC ⁶ using PE ² and markers	<i>Rhodomonas salina</i>	268	NP sufficient N deficient P deficient	0.43 0.71 0.66	15.0 25.0 24.0	12	Carvalho & Granéli, (2010)		
KAC 39	FC ⁶ using PE and markers + PCR	<i>Rhodomonas salina</i>	268	Low N	0.40	14.0	6.7	Bowers et al., (2010)		
CCAP 946/6	Microscopy	<i>Thalassiosira</i> sp.	34	Nutrient depletion	0.75*	3.36	8	Martin-Cereceda et al., (2003)		
		<i>Thalassiosira</i> sp. + bacteria			0.60*	2.69				
		<i>Minidiscus trioculatus</i>	268		0.30*	10.7				
		<i>M. trioculatus</i> + bacteria			0.10*	3.58				
RHPAT89	Microscopy	Fluorescent labeled bacteria (FLB)	1	P deficient P sufficient	3.62 0.97	0.25 0.07	3	Legrand (2001)		
		Fluorescent microspheres (FM)	4	P deficient P sufficient	0.02 0.03	0.09 0.13				
		-								
		¹⁴ C labeling	Bacteria	0.06	Low P	0.7			16.8	20 min

¹IR= Ingestion rate; ²PE= Phycoerythrin; ³FM= Fluorescent microspheres; ⁴FLB= Fluorescent labeled bacteria; ⁵RLB= Radioactive labelled bacteria; ⁶FC = Flow cytometer; *Death rates.

Effects of phosphorus in the form of prey or nutrient on the growth and ingestion rates of *P. parvum*

Phosphorus (P) is an essential element used by all phytoplankton to acquire energy and grow (Benitez-Nelson, 2000). In coastal seawaters, the concentration of phosphate is comprised between 0.1 and 10 μM depending on the period of the year, and often limited, particularly during summer time (Karl & Björkman, 2015). Despite the fact that blooms of *P. parvum* have been predominantly reported in low saline eutrophic coastal waters (Heisler et al., 2008), our study confirmed our first hypothesis by showing that *P. parvum* can grow in a medium without inorganic phosphorus in the presence of other microalgae (i.e. the cryptophyte *Teleaulax amphioxeia*). Thus, the ability to consume dissolved and/or particulate organic matter from other microalgae, may explain why it can forming bloom in coastal waters during summer periods when inorganic nutrient concentrations are very low. Moreover, in the present study we provided a quantitative evidence from a two-week time of experiment, that ingestion of P in the form of living prey increases the growth rate of *P. parvum* compared to the growth rate in monocultures (i.e. with inorganic phosphorus only). This suggests that prey consumption provides some benefits beyond nutrients (proteins, amino acids etc.) which should be confirmed with further investigation.

We hypothesized that the addition of algal prey would allow *P. parvum* to grow under P deficiency conditions as it is expected for constitutive mixotrophs (Mitra et al., 2016), but not under nutrient replete conditions. However, in the presence of sufficiency of inorganic phosphorus and prey, the growth rate was 1.3 times higher than with only prey and about twice as high as with inorganic P only (i.e. strict autotrophy). Our results are in line with those of Brutemark & Granéli, (2011), who achieved higher growth with prey and nutrients than with only nutrients. The higher growth rate may reflect a

combination of the two trophic modes. In fact, when grown under P-sufficiency, phagotrophic activity was still present, but at a lower level compared to P-deficiency (0.25 ± 0.009 vs 0.39 ± 0.008 prey $Pp^{-1} d^{-1}$, after 24h).

On the other hand, if nutrients are present in the medium, prey cells should have a higher P quota. This implies that in P-sufficient cultures, inorganic P assimilation combined with higher P intake per prey can support growth at a maximum P quota level. Additionally, the biochemical composition of prey is also probably different between the treatments (Harrison et al., 1990; Guevara et al., 2016), which could lead to different nutritional intake.

Allelopathic effect of *P. parvum* on *T. amphioxeia*

In mixed culture, *P. parvum* cells negatively affected the growth rate of *T. amphioxeia*, with a higher prey mortality rate induced by lytic compounds and prey ingestion in P-deficient cultures than in the culture with inorganic P. These observations are in accordance with other studies that have shown that lytic effect increases when cells are growing under P-deficient conditions (Barreiro et al., 2005; Uronen et al., 2005; Carvalho & Granéli, 2010; Hambright et al., 2015; Cagle et al., 2021). Moreover, the toxic compounds produced by *P. parvum* not only lead to immobilization of prey cells and subsequently prey ingestion; they can also induce cell lysis of the prey (Skovgaard & Hansen, 2003; Blossom, 2014; Blossom et al., 2014). This implies that *P. parvum* might be able to combine the production of allelopathic compounds and mixotrophy to achieve optimal growth. In addition to organic matter ingestion, toxin production by *P. parvum* may provide some benefit by removing its competitors and grazers. Indeed, it has been previously reported that some phytoplankton groups (Fistarol et al., 2003; Legrand et al., 2003; Uronen et al., 2005;

Michaloudi et al., 2008; Cagle et al., 2021), ciliates (Granéli & Johansson, 2003a), copepods (Nejstgaard & Solberg, 1996; Sapanen et al., 2006), rotifers (Barreiro et al., 2005) and fish (James et al., 2011; Roelke et al., 2011; Taylor et al., 2021) are negatively affected by the presence of *P. parvum* in the medium. It would therefore be interesting to perform a screening of different algae sensitive to the bioactivity of *P. parvum* in order to better understand the relationships within the ecosystems.

Utilization of algal debris by *P. parvum*

During the first and second experiments, a high proportion of lysed prey cells was observed on cytograms. Despite the fact that organic debris may be used by *P. parvum* as food, as far as we know, there is no data in literature highlighting its role in growth. Our study shows that *P. parvum* is able to grow on prey debris in nutrient depleted conditions with a growth rate similar to that obtained in monocultures under nutrient replete conditions. Nevertheless, our results also indicate that the debris of *T. amphioxeia* does not increase the growth of *P. parvum* as much as live prey does. Interestingly, in the presence of nutrients and debris of prey, the rate of inorganic P uptake was lower than without debris, showing that the debris are a source of P for *P. parvum* even in the presence of inorganic P. However, it should be noted that different processes can be at stake: phagotrophy of debris, osmotrophy of small molecules, and P remineralization by bacteria or by *P. parvum* alkaline phosphatases. Further experiments are required, using techniques such as isotopes (Carpenter et al., 2018), to better assess the contribution of trophic fluxes in *P. parvum*. Finally, experiments measuring the activity of alkaline phosphatases (Beardall et al., 2001) will allow a more accurate estimation of nature of phosphorus consumed by *P. parvum* from the debris.

Conclusion

We developed a method that takes digestion rate into account allowing the calculation of ingestion rates over a two-week period, when predators are used to prey and balanced mixotrophic growth is reached. Interestingly, this study demonstrated that feeding on living prey can significantly increase the growth rate of *P. parvum* and that *P. parvum* is able to utilize recently formed algal debris to grow. The present study also highlights the link between phagotrophy, allelopathy and growth in *P. parvum*. To improve our model, further studies are required to estimate more accurately the rate of prey digestion. These data may be used to improve existing models (Litchman, 2023; Mitra et al., 2023) on trophic modes and more widely on mixotrophy in oceans.

Acknowledgments

This work was supported by LEFE through the HeteroMixo Project. The authors acknowledge the Cytocell - Flow Cytometry and FACS core facility (SFR Bonamy, BioCore, Inserm UMS 016, CNRS UAR 3556, Nantes, France) for its technical expertise and help, member of the Scientific Interest Group (GIS) Biogenouest and the Labex IGO program supported by the French National Research Agency (n°ANR-11-LABX-0016-01). We acknowledge the IBISA MicroPICell facility (Biogenouest), member of the national infrastructure France-Bioimaging supported by the French national research agency (ANR-10-INBS-04). The authors thank Clarisse Hubert for her contribution to the nutrient analysis.

References

- Adolf, J. E., Bachvaroff, T., & Place, A. R. (2008). Can cryptophyte abundance trigger toxic *Karlodinium veneficum* blooms in eutrophic estuaries? *Harmful Algae*, 8(1), 119-128. <https://doi.org/10.1016/j.hal.2008.08.003>
- Almada, E. V. C., Carvalho, W. F. de, & Nascimento, S. M. (2017). Investigation of phagotrophy in natural assemblages of the benthic dinoflagellates *Ostreopsis*, *Prorocentrum* and *Coolia*. *Brazilian Journal of Oceanography*, 65(3), 392-399. <https://doi.org/10.1590/s1679-87592017140706503>
- Anestis, K., Wohlrab, S., Varga, E., Hansen, P. J., & John, U. (2022). The relationship between toxicity and mixotrophy in bloom dynamics of the ichthyotoxic *Prymnesium parvum* [Preprint]. Preprints. <https://doi.org/10.22541/au.166427474.41023349/v1>
- Baker, J. W., Grover, J. P., Brooks, B. W., Ureña-Boeck, F., Roelke, D. L., Errera, R., & Kiesling, R. L. (2007). Growth and Toxicity of *Prymnesium Parvum* (haptophyta) as a Function of Salinity, Light, and Temperature¹. *Journal of Phycology*, 43(2), 219-227. <https://doi.org/10.1111/j.1529-8817.2007.00323.x>
- Barreiro, A., Guisande, C., Maneiro, I., Lien, T., Legrand, C., Tamminen, T., Lehtinen, S., Uronen, P., & Granéli, E. (2005). Relative importance of the different negative effects of the toxic haptophyte *Prymnesium parvum* on *Rhodomonas salina* and *Brachionus plicatilis*. *Aquatic Microbial Ecology*, 38, 259-267. <https://doi.org/10.3354/ame038259>
- Beardall, J., Young, E., & Roberts, S. (2001). Approaches for determining phytoplankton nutrient limitation. *Aquatic Sciences*, 63(1), 44-69. <https://doi.org/10.1007/PL00001344>
- Beisner, B. E., Grossart, H.-P., & Gasol, J. M. (2019). A guide to methods for estimating phago-mixotrophy in nanophytoplankton. *Journal of Plankton Research*, 41(2), 77-89. <https://doi.org/10.1093/plankt/fbz008>
- Benitez-Nelson, C. R. (2000). The biogeochemical cycling of phosphorus in marine systems. *Earth-Science Reviews*, 51(1-4), 109-135. [https://doi.org/10.1016/S0012-8252\(00\)00018-0](https://doi.org/10.1016/S0012-8252(00)00018-0)
- Blossom, H. E. (2014). *Prymnesium parvum* revisited: Relationship between allelopathy, ichthyotoxicity, and chemical profiles in 5 strains. *Aquatic Toxicology*, 8.
- Blossom, H. E., Andersen, N., Hansen, P., & Rasmussen, S. (2014). Stability of the intra- and extracellular toxins of *Prymnesium parvum* using a microalgal bioassay. [https://doi.org/10.1016/S1568-9883\(03\)00006-4](https://doi.org/10.1016/S1568-9883(03)00006-4)
- Bowers, H. A., Brutemark, A., Carvalho, W. F., & Granéli, E. (2010). Combining Flow Cytometry and Real-Time PCR Methodology to Demonstrate Consumption by *Prymnesium parvum*¹. *JAWRA Journal of the American Water Resources Association*, 46(1), 133-143. <https://doi.org/10.1111/j.1752-1688.2009.00397.x>
- Brutemark, A., & Granéli, E. (2011). Role of mixotrophy and light for growth and survival of the toxic haptophyte *Prymnesium parvum*. *Harmful Algae*, 10(4), 388-394. <https://doi.org/10.1016/j.hal.2011.01.005>
- Burkholder, J. M., Glibert, P. M., & Skelton, H. M. (2008). Mixotrophy, a major mode of nutrition for harmful algal species in eutrophic waters. *Harmful Algae*, 8(1), 77-93. <https://doi.org/10.1016/j.hal.2008.08.010>

- Cagle, S. E., Roelke, D. L., & Muhl, R. W. (2021). Allelopathy and micropredation paradigms reconcile with system stoichiometry. *Ecosphere*, 12(2), e03372. <https://doi.org/10.1002/ecs2.3372>
- Carpenter, K. J., Bose, M., Polerecky, L., Lie, A. A. Y., Heidelberg, K. B., & Caron, D. A. (2018). Single-Cell View of Carbon and Nitrogen Acquisition in the Mixotrophic Alga *Prymnesium parvum* (Haptophyta) Inferred From Stable Isotope Tracers and NanoSIMS. *Frontiers in Marine Science*, 5, 157. <https://doi.org/10.3389/fmars.2018.00157>
- Carvalho, W. F., & Granéli, E. (2010). Contribution of phagotrophy versus autotrophy to *Prymnesium parvum* growth under nitrogen and phosphorus sufficiency and deficiency. *Harmful Algae*, 9(1), 105-115. <https://doi.org/10.1016/j.hal.2009.08.007>
- Driscoll, W. W., Wisecaver, J. H., Hackett, J. D., Espinosa, N. J., Padway, J., Engers, J. E., & Bower, J. A. (2023). Behavioural differences underlie toxicity and predation variation in blooms of *Prymnesium parvum*. *Ecology Letters*, 26(5), 677-691. <https://doi.org/10.1111/ele.14172>
- Edvardsen, B., & Paasche, E. (1998). Bloom Dynamics and Physiology of *Prymnesium* and *Chrysochromulina* (p. 193-208).
- Edwards, K. F. (2019). Mixotrophy in nanoflagellates across environmental gradients in the ocean. *Proceedings of the National Academy of Sciences*, 116(13), 6211-6220. <https://doi.org/10.1073/pnas.1814860116>
- Ferreira, G. D., Figueira, J., Marques, S. C., Hansen, P. J., & Calbet, A. (2022). The strengths and weaknesses of Live Fluorescently Labelled Algae (LFLA) to estimate herbivory in protozooplankton and mixoplankton. *Marine Environmental Research*, 174, 105558. <https://doi.org/10.1016/j.marenvres.2022.105558>
- Fistarol, G., Legrand, C., & Granéli, E. (2003). Allelopathic effect of *Prymnesium parvum* on a natural plankton community. *Marine Ecology Progress Series*, 255, 115-125. <https://doi.org/10.3354/meps255115>
- Flynn, K. J., Mitra, A., Glibert, P. M., & Burkholder, J. M. (2018). Mixotrophy in Harmful Algal Blooms: By Whom, on Whom, When, Why, and What Next. In P. M. Glibert, E. Berdalet, M. A. Burford, G. C. Pitcher, & M. Zhou (Éds.), *Global Ecology and Oceanography of Harmful Algal Blooms* (p. 113-132). Springer International Publishing. https://doi.org/10.1007/978-3-319-70069-4_7
- Flynn, K. J., Stoecker, D. K., Mitra, A., Raven, J. A., Glibert, P. M., Hansen, P. J., Granéli, E., & Burkholder, J. M. (2013). Misuse of the phytoplankton–zooplankton dichotomy: The need to assign organisms as mixotrophs within plankton functional types. *Journal of Plankton Research*, 35(1), 3-11. <https://doi.org/10.1093/plankt/fbs062>
- Granéli, E., & Johansson, N. (2003a). Effects of the toxic haptophyte *Prymnesium parvum* on the survival and feeding of a ciliate: The influence of different nutrient conditions. *Marine Ecology Progress Series*, 254, 49-56. <https://doi.org/10.3354/meps254049>
- Granéli, E., & Johansson, N. (2003b). Increase in the production of allelopathic substances by *Prymnesium parvum* cells grown under N- or P-deficient conditions. *Harmful Algae*, 2(2), 135-145. [https://doi.org/10.1016/S1568-9883\(03\)00006-4](https://doi.org/10.1016/S1568-9883(03)00006-4)

- Granéli, E., & Salomon, P. S. (2010). Factors Influencing Allelopathy and Toxicity in *Prymnesium parvum*. *JAWRA Journal of the American Water Resources Association*, 46(1), 108-120. <https://doi.org/10.1111/j.1752-1688.2009.00395.x>
- Guevara, M., Arredondo-Vega, B. O., Palacios, Y., Saéz, K., & Gómez, P. I. (2016). Comparison of growth and biochemical parameters of two strains of *Rhodomonas salina* (Cryptophyceae) cultivated under different combinations of irradiance, temperature, and nutrients. *Journal of Applied Phycology*, 28(5), 2651-2660. <https://doi.org/10.1007/s10811-016-0835-2>
- Hambright, K. D., Easton, J. D., Zamor, R. M., Beyer, J., Easton, A. C., & Allison, B. (2015). Regulation of growth and toxicity of a mixotrophic microbe: Implications for understanding range expansion in *Prymnesium parvum*. *Freshwater Science*. <https://doi.org/10.1086/677198>
- Harrison, P. J., Thompson, P. A., & Calderwood, G. S. (1990). Effects of nutrient and light limitation on the biochemical composition of phytoplankton. *Journal of Applied Phycology*, 2(1), 45-56. <https://doi.org/10.1007/BF02179768>
- Hartmann, M., Grob, C., Tarran, G. A., Martin, A. P., Burkill, P. H., Scanlan, D. J., & Zubkov, M. V. (2012). Mixotrophic basis of Atlantic oligotrophic ecosystems. *Proceedings of the National Academy of Sciences*, 109(15), 5756-5760. <https://doi.org/10.1073/pnas.1118179109>
- Heisler, J., Glibert, P., Burkholder, J., Anderson, D., Cochlan, W., Dennison, W., Gobler, C., Dortch, Q., Heil, C., Humphries, E., Lewitus, A., Magnien, R., Marshall, H., Sellner, K., Stockwell, D., Stoecker, D., & Suddleson, M. (2008). Eutrophication and Harmful Algal Blooms: A Scientific Consensus. *Harmful Algae*, 8(1), 3-13. <https://doi.org/10.1016/j.hal.2008.08.006>
- Henrikson, J. C., Gharfeh, M. S., Easton, A. C., Easton, J. D., Glenn, K. L., Shadfan, M., Mooberry, S. L., Hambright, K. D., & Cichewicz, R. H. (2010). Reassessing the ichthyotoxin profile of cultured *Prymnesium parvum* (golden algae) and comparing it to samples collected from recent freshwater bloom and fish kill events in North America. *Toxicon*, 55(7), 1396-1404. <https://doi.org/10.1016/j.toxicon.2010.02.017>
- James, S. V., Valenti, T. W., Prosser, K. N., Grover, J. P., Roelke, D. L., & Brooks, B. W. (2011). Sunlight amelioration of *Prymnesium parvum* acute toxicity to fish. *Journal of Plankton Research*, 33(2), 265-272. <https://doi.org/10.1093/plankt/fbq082>
- Johnsen, T. M., Eikrem, W., Olseng, C. D., Tollefsen, K. E., & Bjerknes, V. (2010). *Prymnesium parvum*: The Norwegian Experience. *JAWRA Journal of the American Water Resources Association*, 46(1), 6-13. <https://doi.org/10.1111/j.1752-1688.2009.00386.x>
- Karl, D. M., & Björkman, K. M. (2015). Dynamics of Dissolved Organic Phosphorus. In *Biogeochemistry of Marine Dissolved Organic Matter* (p. 233-334). Elsevier. <https://doi.org/10.1016/B978-0-12-405940-5.00005-4>
- Legrand, C. (2001). Phagotrophy and toxicity variation in the mixotrophic *Prymnesium patelliferum* (Haptophyceae). *Limnology and Oceanography*, 46(5), 1208-1214. <https://doi.org/10.4319/lo.2001.46.5.1208>
- Legrand, C., Rengefors, K., Fistarol, G. O., & Granéli, E. (2003). Allelopathy in phytoplankton—Biochemical, ecological and evolutionary aspects. *Phycologia*, 42(4), 406-419. <https://doi.org/10.2216/i0031-8884-42-4-406.1>

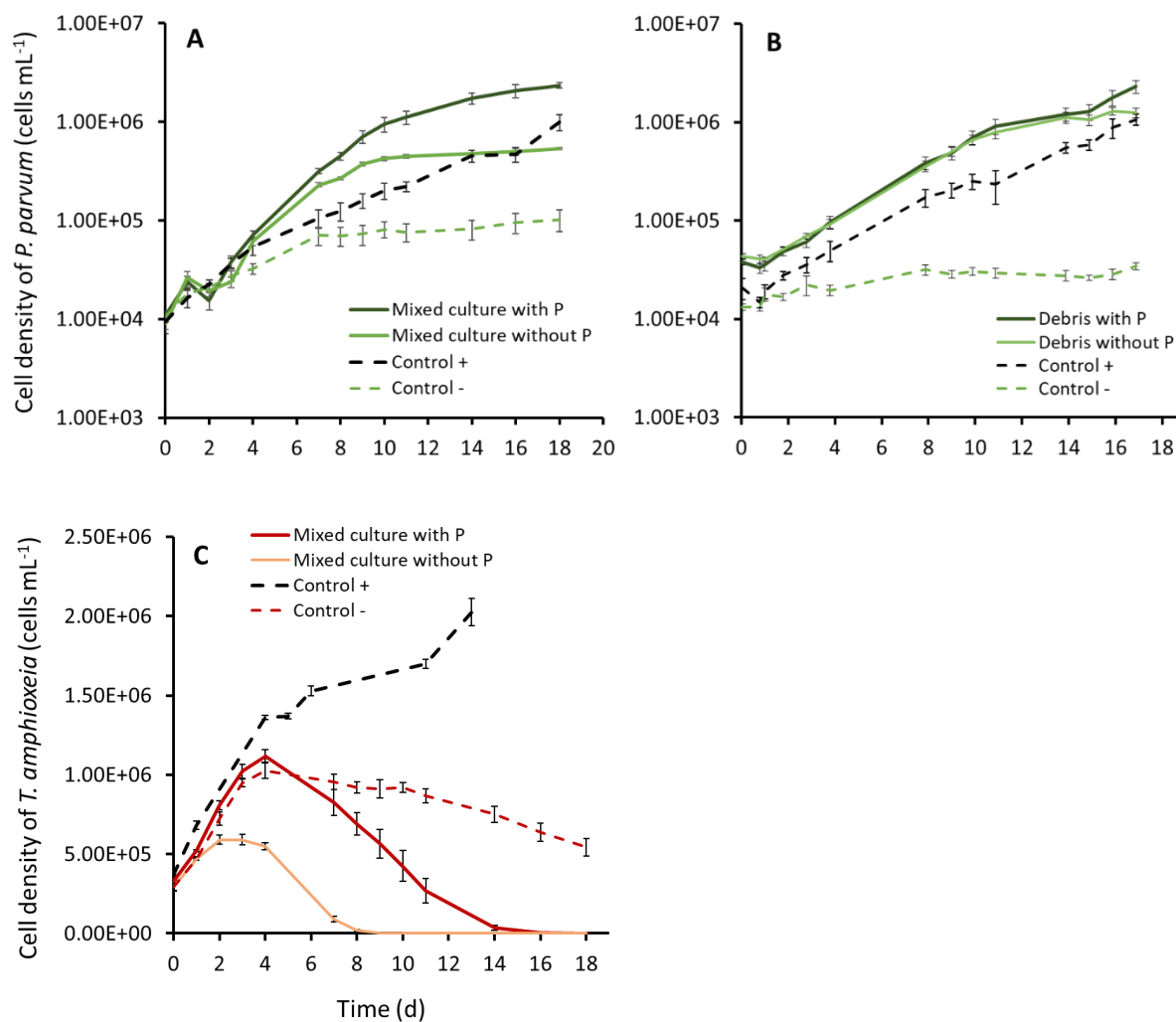
- Li, M., Chen, Y., Zhang, F., Song, Y., Glibert, P. M., & Stoecker, D. K. (2022). A three-dimensional mixotrophic model of *Karlodinium veneficum* blooms for a eutrophic estuary. *Harmful Algae*, 113, 102203. <https://doi.org/10.1016/j.hal.2022.102203>
- Litchman, E. (2023). Understanding and predicting harmful algal blooms in a changing climate : A trait-based framework. *Limnology and Oceanography Letters*, 8(2), 229-246. <https://doi.org/10.1002/lol2.10294>
- Lundgren, V. M., Glibert, P. M., Granéli, E., Vidyarathna, N. K., Fiori, E., Ou, L., Flynn, K. J., Mitra, A., Stoecker, D. K., & Hansen, P. J. (2016). Metabolic and physiological changes in *Prymnesium parvum* when grown under, and grazing on prey of, variable nitrogen:phosphorus stoichiometry. *Harmful Algae*, 55, 1-12. <https://doi.org/10.1016/j.hal.2016.01.002>
- Marchowski, D., & Ławicki, Ł. (2023). Unprecedented mass mortality of aquatic organisms in the River Oder. *Oryx*, 57(1), 9-9. <https://doi.org/10.1017/S0030605322001387>
- Martin-Cereceda, M., Novarino, G., & Young, J. (2003). Grazing by *Prymnesium parvum* on small planktonic diatoms. *Aquatic Microbial Ecology*, 33, 191-199. <https://doi.org/10.3354/ame033191>
- Matantseva, O. V., & Skarlato, S. O. (2013). Mixotrophy in microorganisms : Ecological and cytophysiological aspects. *Journal of Evolutionary Biochemistry and Physiology*, 49(4), 377-388. <https://doi.org/10.1134/S0022093013040014>
- Medić, N., Varga, E., Waal, D. B. V. de, Larsen, T. O., & Hansen, P. J. (2022). The coupling between irradiance, growth, photosynthesis and prymnesin cell quota and production in two strains of the bloom-forming haptophyte, *Prymnesium parvum*. *Harmful Algae*, 112, 102173. <https://doi.org/10.1016/j.hal.2022.102173>
- Michaloudi, E., Moustaka-Gouni, M., Gkelis, S., & Pantelidakis, K. (2008). Plankton community structure during an ecosystem disruptive algal bloom of *Prymnesium parvum*. *Journal of Plankton Research*, 31(3), 301-309. <https://doi.org/10.1093/plankt/fbn114>
- Mitra, A., Caron, D. A., Faure, E., Flynn, K. J., Leles, S. G., Hansen, P. J., McManus, G. B., Not, F., do Rosario Gomes, H., Santoferrara, L. F., Stoecker, D. K., & Tillmann, U. (2023). The Mixoplankton Database (MDB) : Diversity of photo-phago-trophic plankton in form, function, and distribution across the global ocean. *Journal of Eukaryotic Microbiology*, n/a(n/a), e12972. <https://doi.org/10.1111/jeu.12972>
- Mitra, A., Flynn, K. J., Burkholder, J. M., Berge, T., Calbet, A., Raven, J. A., Granéli, E., Glibert, P. M., Hansen, P. J., Stoecker, D. K., Thingstad, F., Tillmann, U., Våge, S., Wilken, S., & Zubkov, M. V. (2014). The role of mixotrophic protists in the biological carbon pump. *Biogeosciences*, 11(4), 995-1005. <https://doi.org/10.5194/bg-11-995-2014>
- Mitra, A., Flynn, K. J., Tillmann, U., Raven, J. A., Caron, D., Stoecker, D. K., Not, F., Hansen, P. J., Hallegraeff, G., Sanders, R., Wilken, S., McManus, G., Johnson, M., Pitta, P., Våge, S., Berge, T., Calbet, A., Thingstad, F., Jeong, H. J., ... Lundgren, V. (2016). Defining Planktonic Protist Functional Groups on Mechanisms for Energy and Nutrient Acquisition : Incorporation of Diverse Mixotrophic Strategies. *Protist*, 167(2), 106-120. <https://doi.org/10.1016/j.protis.2016.01.003>
- Nejstgaard, J. C., & Solberg, P. T. (1996). Repression of copepod feeding and fecundity by the toxic haptophyte *Prymnesium patelliferum*. *Sarsia*, 81(4), 339-344. <https://doi.org/10.1080/00364827.1996.10413631>

- Nygaard, K., & Tobiesen, A. (1993). Bacterivory in algae : A survival strategy during nutrient limitation. *Limnology and Oceanography*, 38(2), 273-279. <https://doi.org/10.4319/lo.1993.38.2.0273>
- Pujo-Pay, M., & Raimbault, P. (1994). Improvement of the wet-oxidation procedure for simultaneous determination of particulate organic nitrogen and phosphorus collected on filters. *Marine Ecology Progress Series*, 105, 203-207. <https://doi.org/10.3354/meps105203>
- Roelke, D. L., Barkoh, A., Brooks, B. W., Grover, J. P., Hambright, K. D., LaClaire, J. W., Moeller, P. D. R., & Patino, R. (2016). A chronicle of a killer alga in the west : Ecology, assessment, and management of *Prymnesium parvum* blooms. *Hydrobiologia*, 764(1), 29-50. <https://doi.org/10.1007/s10750-015-2273-6>
- Roelke, D. L., Grover, J. P., Brooks, B. W., Glass, J., Buzan, D., Southard, G. M., Fries, L., Gable, G. M., Schwierzke-Wade, L., Byrd, M., & Nelson, J. (2011). A decade of fish-killing *Prymnesium parvum* blooms in Texas : Roles of inflow and salinity. *Journal of Plankton Research*, 33(2), 243-253. <https://doi.org/10.1093/plankt/fbq079>
- Skovgaard, A., & Hansen, P. J. (2003). Food uptake in the harmful alga *Prymnesium parvum* mediated by excreted toxins. *Limnology and Oceanography*, 48(3), 1161-1166. <https://doi.org/10.4319/lo.2003.48.3.1161>
- Smalley, G., Coats, D., & Adam, E. (1999). A new method using fluorescent microspheres to determine grazing on ciliates by the mixotrophic dinoflagellate *Ceratium furca*. *Aquatic Microbial Ecology*, 17, 167-179. <https://doi.org/10.3354/ame017167>
- Sopanen, S., Koski, M., Kuuppo, P., Uronen, P., Legrand, C., & Tamminen, T. (2006). Toxic haptophyte *Prymnesium parvum* affects grazing, survival, egestion and egg production of the calanoid copepods *Eurytemora affinis* and *Acartia bifilosa*. *Marine Ecology Progress Series*, 327, 223-232. <https://doi.org/10.3354/meps327223>
- Stoecker, D. K., Hansen, P. J., Caron, D. A., & Mitra, A. (2017). Mixotrophy in the Marine Plankton. *Annual Review of Marine Science*, 9(1), 311-335. <https://doi.org/10.1146/annurev-marine-010816-060617>
- Taylor, R. B., Hill, B. N., Langan, L. M., Chambliss, C. K., & Brooks, B. W. (2021). Sunlight concurrently reduces *Prymnesium parvum* elicited acute toxicity to fish and prymnesins. *Chemosphere*, 263, 127927. <https://doi.org/10.1016/j.chemosphere.2020.127927>
- Tillmann, U. (1998). Phagotrophy by a plastidic haptophyte, *Prymnesium patelliferum*. *Aquatic Microbial Ecology*, 14(2), 155-160. <https://doi.org/10.3354/ame014155>
- Unrein, F., Gasol, J. M., Not, F., Forn, I., & Massana, R. (2014). Mixotrophic haptophytes are key bacterial grazers in oligotrophic coastal waters. *The ISME Journal*, 8(1), Article 1. <https://doi.org/10.1038/ismej.2013.132>
- Uronen, P., Kuuppo, P., Legrand, C., & Tamminen, T. (2007). Allelopathic Effects of Toxic Haptophyte *Prymnesium parvum* Lead to Release of Dissolved Organic Carbon and Increase in Bacterial Biomass. *Microbial Ecology*, 54(1), 183-193. <https://doi.org/10.1007/s00248-006-9188-8>
- Uronen, P., Lehtinen, S., Legrand, C., Kuuppo, P., & Tamminen, T. (2005). Haemolytic activity and allelopathy of the haptophyte *Prymnesium parvum* in nutrient-limited and balanced

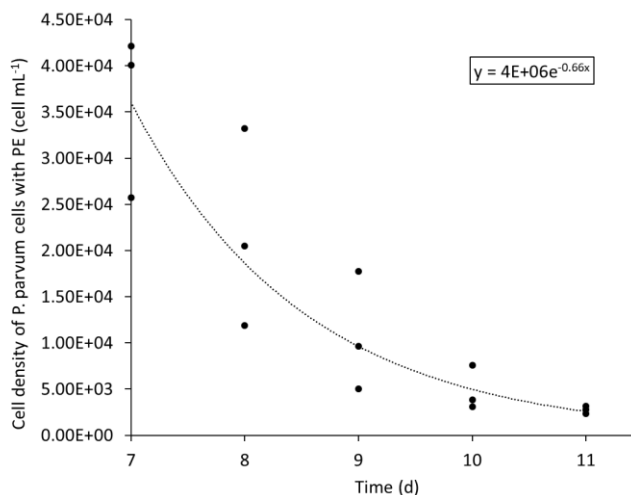
growth conditions. *Marine Ecology Progress Series*, 299, 137-148. <https://doi.org/10.3354/meps299137>

Yoo, Y. D., Seong, K. A., Jeong, H. J., Yih, W., Rho, J.-R., Nam, S. W., & Kim, H. S. (2017). Mixotrophy in the marine red-tide cryptophyte *Teleaulax amphioxeia* and ingestion and grazing impact of cryptophytes on natural populations of bacteria in Korean coastal waters. *Harmful Algae*, 68, 105-117. <https://doi.org/10.1016/j.hal.2017.07.012>

Supplementary figures (+ movie)



Supplementary Fig. 1. Cell densities (cells mL⁻¹) of *Prymnesium parvum* grown in monoculture with and without inorganic phosphorus (Ctrl +IP, Ctrl -IP, dashed lines), (A) with living cells of prey in presence or absence of inorganic phosphorus (Prey +IP, Prey -IP, solid lines, exp. 2), and (B) with debris of *Teleaulax amphioxeia* with or without inorganic phosphorus, (Debris +IP, Debris -IP, solid lines, exp. 3). (C) *Teleaulax amphioxeia* cell densities grown in monoculture with and without inorganic phosphorus (Ctrl +IP, Ctrl -IP, dashed lines) and with living cells of predators (*Prymnesium parvum*) in presence or absence of inorganic phosphorus (Prey +IP, Prey -IP, solid lines, exp. 2). Values are mean \pm SD, n = 3.



Supplementary Fig. 2. Disappearance of feeding cells of *Prymnesium parvum* (cells of *P. parvum* with PE fluorescence, cells mL⁻¹) when the stock of prey (*Teleaulax amphioxeia*) is depleted in absence of inorganic phosphorus (Prey -IP). Focusing on the period when there is no more prey in the Prey -P treatment (from day 7), a digestion rate of 0.66 d⁻¹ was observed.

Supplementary Tab. 1. Statistical data of normality (Shapiro-Wilk) and homoscedasticity (Bartlett) test and the result of the ANOVA according to the treatment. When p-value >0.05 for Shapiro-Wilk test, the residuals of the model are normally distributed and for Bartlett test, the data are homogeneous. When p-value <0.05 for the ANOVA, there is a significant difference between the groups.

Treatment name	Normality (Shapiro-Wilk)	Homoscedasticity (Barlett test)	ANOVA
Mixed cultures with living prey	0.49	0.62	3.25 10 ⁻⁴
Monocultures with prey debris	0.13	0.94	1.97 10 ⁻³
Prey growth rates	0.54	0.23	1.72 10 ⁻⁶